Propellants, Explosives, Pyrotechnics

WILEY-VCH

Propellants, Explosives, Pyrotechnics

RESEARCH ARTICLE OPEN ACCESS

The Use of Chemiluminescence Nitrogen Oxides Analysis for the Study of the Decomposition of Nitrocellulose

Ian Wallace[1] | Nathalie Mai[1] | Philip Gill[1,2] | Rudi Hood[1] | Matt Parker[1] | Libby Napper[1]

[1]Centre for Defence Chemistry, Defence Academy of the United Kingdom, Cranfield University, Shrivenham, UK | [2]Roxel (UK Rocket Motors) Ltd, Kidderminster, UK

Correspondence: Ian Wallace (i.g.wallace@cranfield.ac.uk)

Received: 17 October 2024 | **Accepted:** 10 February 2025

Keywords: activation energy | chemiluminescence | decomposition kinetics | nitrocellulose | nitrogen oxides

ABSTRACT

Understanding the decomposition of nitrocellulose (NC) and other nitrate esters within storage and usage temperature ranges is essential for managing the service life and safety of (NC)-containing formulations. High-temperature decomposition studies often fail to reflect typical storage conditions due to temperature-dependent mechanisms. This study uses chemiluminescence nitrogen oxides (NO_x) analysers to examine NC decomposition, measuring NO_x evolution across a wide temperature range. From 20°C to 135°C, decomposition modes include thermolysis, hydrolysis, and physical desorption. Results show NO_x can desorb from NC at ambient temperatures, potentially misleading traditional stability tests. The quantity of NO_x generated depends on material history and can be reduced by pre-test procedures. While thermolysis dominates at higher temperatures with an activation energy of 140 $kJ.mol^{-1}$, hydrolysis is predominant at lower temperatures with an activation energy of 46 $kJ.mol^{-1}$. This low activation energy should be considered in any life assessment predictions. In this lower temperature regime, moisture significantly affects decomposition rates, especially below 50°C. Whilst the rate increases in the presence of moisture, the activation energy for the hydrolysis process is unaffected. Chemiluminescence NO_x analysis has proven to be a powerful tool for studying the low-temperature decomposition behaviours of NC and NC-containing formulations. This innovative approach not only enhances the understanding of NC decomposition but also offers a more efficient and accurate method for assessing the stability of NC-containing formulations.

1 | Introduction

Nitrocellulose (NC) is manufactured by the nitration of cellulose, usually from natural sources such as wood or cotton [1]. It has been used in a range of applications, including as a thermoplastic film, in paints and lacquers [2], inks [3] and adhesives [4], recently in Coronavirus disease test kits [5] and historically as photographic film [6]. At high levels of nitration (12.2%–13.9%), NC is used in the manufacture of rocket and gun propellants, sometimes as the principal energetic ingredient and sometimes in conjunction with other nitrate esters such as nitro-glycerine in double-based propellants or additionally, with nitroguanidine in triple-based propellants. NC has also been used as an energetic binder in some high-explosive formulations. Its major advantage as a rocket motor propellant is that it does not generate smoke during combustion. Its major disadvantage is that, as a nitrate ester, it is liable to decompose even at low temperatures generating reaction products that can further accelerate the decomposition. This autocatalytic process can lead to thermal runaway and has been the likely cause of several major explosions, such as the explosion in Tianjin in China in 2015 which is reported to have killed 173 people and injured many more [7]. The top causative event was attributed to the spontaneous ignition of NC [8]. NC-based formulations, therefore, include chemical

https://doi.org/10.1002/prep.12040

TABLE 1 | Comparison of high-temperature nitrocellulose (NC) decomposition activation energies by different methods.

Date	NC [%N, w/w]	Temp. [°C]	Method	E_a [kJ/mol]	Ref.
2004	—	—	Nitrate Bond dissociation energies	134–164	[14]
1981	12.0	90–135	NO_x chemiluminescence	179.8	[10]
1980	12.6	55–135	NO_x chemiluminescence	141.2	[11]
1955	13.9	142–172	Infra-red	192.5	[12]
1955	13.9	142–172	Weight loss	180.66	[12]
1900	13.1–13.45	126.5–157	Gas evolution	193.3	[13]

stabilisers that react with the decomposition products and, whilst they remain, they prevent the autocatalytic reactions that cause self-heating and potential ignition. However, chemical stabilisers do not prevent the underlying process of decomposition but manage its effects.

To manage the service and safe life of NC-containing formulations, it is important to understand the underlying decomposition of NC and, indeed, other nitrate esters, especially in the temperature range in which they are stored and deployed. At ambient storage temperatures, the decomposition behaviour is almost imperceptible, and hence much work in this area has been conducted at elevated temperatures where measurable rates of change in, for example, stabiliser consumption, heat generation or gas evolution, can be measured. With a knowledge of chemical kinetics, it is possible to extrapolate behaviour to lower, more realistic temperatures. This assumes that the degradation mechanisms that pertain to higher temperatures also dominate in the low-temperature regime. That is not a safe assumption [9].

At elevated temperatures, the decomposition rates of NC have been measured [10–13] using a variety of methods including direct measurement of oxides of nitrogen release, infrared, mass loss, and volume of gas generated. The calculated activation energies are listed in Table 1. The literature concludes that the dominant reaction is the thermolysis of the $O—NO_2$ bond, releasing nitrogen dioxide (NO_2), which is thought to be rapidly reduced to nitric oxide (NO). The activation energy for this thermolytic cleavage of the $O—NO_2$ has been measured and is believed to be in the range of 140–180 kJ/mol. This is consistent with the $O—NO_2$ bond dissociation energies calculated by Khrapkovskii et al. [14].

The widely recognised reaction scheme in the higher temperature region is believed to follow the reaction sequence described by Brill et al. [15] and Kimera [16] and shows a three-step process consistent with:

$$RO - NO_2 \rightarrow RO + NO_2 \rightarrow \text{(Initiation)} \tag{1}$$

$$RO + NO_2 \rightarrow ROO + NO \rightarrow \text{(Propagation)} \tag{2}$$

$$2ROO \rightarrow (R'C = O)^* + O_2{}^* + ROH \rightarrow \text{(Termination)} \tag{3}$$

The fast propagation reaction accounts for observation in experiments where gas is swept through the NC, and NO is the dominant gaseous product. If the pressure in the vicinity of the reactant NC is reduced, the total quantity of nitrogen oxides (NO_x) remains the same, but the proportion of NO_2 increases in the product gases [10]. This is attributed to a back reaction of NO_2 with NC the rate of which depends on the partial pressure of NO_2.

Few studies of NC decomposition at lower temperatures, at and near ambient, have been conducted. However, Volltrauer et al. [10] and Kimura [16] have suggested that the thermolysis process contributes less to decomposition and that the hydrolysis reaction becomes the dominant mode of decomposition. Arrhenius plots have shown a lower activation energy than that observed at temperatures greater than 80°C [10].

Table 2 summarises the activation energies for NC calculated at lower temperatures <80°C using two different chemiluminescence techniques.

The hydrolysis reaction sequence [17] in this instance is thought to be catalysed by the presence of water, as shown:

$$R - O - NO_2 + H_2O \rightarrow ROH + HNO_3 \tag{4}$$

$$R - OH + HNO_3 \rightarrow R^*{-}CHO + NO_2 + H_2O \tag{5}$$

$$R - O - NO_2 \rightarrow RO + NO_2 \tag{6}$$

Again, NO_2 is a product of these reactions and will react through equation (2) to form NO. Hence, measuring the rate of evolution of NO and NO_2 from NC is a useful method to determine the material's decomposition rate. Several authors [10, 11, 18] have used it to assess NC decomposition rates, and those of other nitrate esters, and their formulations.

Under closed conditions, the reaction products of decomposition can react further with the reactants and may catalyse additional reactions to a point where autocatalysis results in self-heating, which can lead to ignition and catastrophic results. Many studies [10, 19, 20, 21], have been conducted to look at the sequence of reactions once NO_x has been produced. However, few studies have focused on the initial reaction that produces NO_x and other products.

This study looks at the modes of NO_x production from NC utilising chemiluminescence NO_x analysers and examines some of the factors that influence NO_x production. These are open-system studies focussed on the forward reactions and should

TABLE 2 | Comparison of low-temperature nitrocellulose (NC) decomposition activation energies by different methods.

Date	NC [%N, w/w]	Temp. [°C]	Method	E_a [kJ/mol]	Ref.
1981	12.0	25–80	NO_x Chemiluminescence	107.1	[10]
1989	12.6	40–90	ROO. Chemiluminescence	58.6	[16]

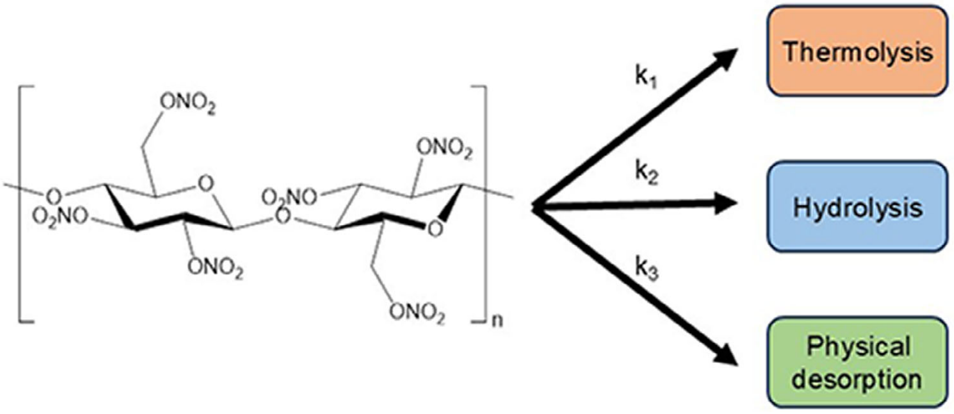

FIGURE 1 | Modes of nitrogen oxides (NO_x) evolution from nitrocellulose (NC).

not be read across to closed systems where a sequence of further reactions will be involved. Three different modes of NO_x evolution have been observed, as illustrated in Figure 1 as a product of the direct chemical decomposition of NC via the mechanisms of (i) thermolysis (>80°C), (ii) hydrolysis (<80°C) or (iii) NO_x gases physically adsorbed within the NC material from a historical decomposition process.

2 | Experimental

2.1 | Chemiluminescence NO_x Analyser

The chemiluminescence technique depends on the reaction between NO and ozone (O_3). The NO is oxidised to NO_2, and O_3 is reduced to oxygen (O_2). The NO_2 formed is in an excited state and releases light when falling back to the ground state. The light produced can be measured and is directly proportional to the quantity of NO present.

$$NO + O_3 \rightarrow NO_2^* + O_2 \tag{7}$$

$$NO_2^* \rightarrow NO_2 + h\upsilon \tag{8}$$

To measure NO_2, the gas stream is diverted through a catalytic or photolytic converter that reduces any NO_2 present to NO. In converter mode, NO_2 and NO are measured together as NO_x. When the converter is bypassed, only NO is measured; hence, NO_2 is determined by difference.

$$[NO_2] = [NO_x] - [NO]$$

This method is capable of measuring parts per trillion levels of NO and NO_2 at temperatures at, and a little above, the temperatures encountered by explosives in storage or deployment. The swept experiment approach is similar to that applied by Will [13], who used carbon dioxide to sweep product gases from NC decomposing at 135°C. The optimal flow is rapid enough to avoid significant back reactions of reaction products with the reactant but not too rapid a flow rate to induce cooling of the sample.

2.2 | Flow Reactor

Our application uses pure nitrogen as the carrier gas at flow rates between 25 and 50 mL/min. The reactor consists of a glass vessel containing a glass sinter that supports the sample. Two different volumes of the reactor (25 and 50 mL) are used to accommodate up to 5 g of fibrous NC.

The reactors can be inserted into a block oven with brass inserts manufactured to provide a snug fit. The block oven can be maintained at a constant temperature or can be controlled to increase at a predetermined rate.

Calibration gases of 1 ppm NO and 1 ppm NO_2 in N_2 are used to calibrate the instrument.

For the kinetics experiments, the 25% water-wetted 12.6% nitrogen NC is dried initially in air and then under vacuum at 60°C for 2 h and then stored in a desiccator. Immediately prior to conducting decomposition experiments, the NC was dried again for 1–2 h in the N_2 gas flow.

All relevant experimental parameters are recorded through a suite of data-logging modules to enable subsequent analysis.

2.3 | Experimental Setup

The schematic of the experimental facility is shown in Figure 2. The flow reactor and NC sample are placed in a block oven,

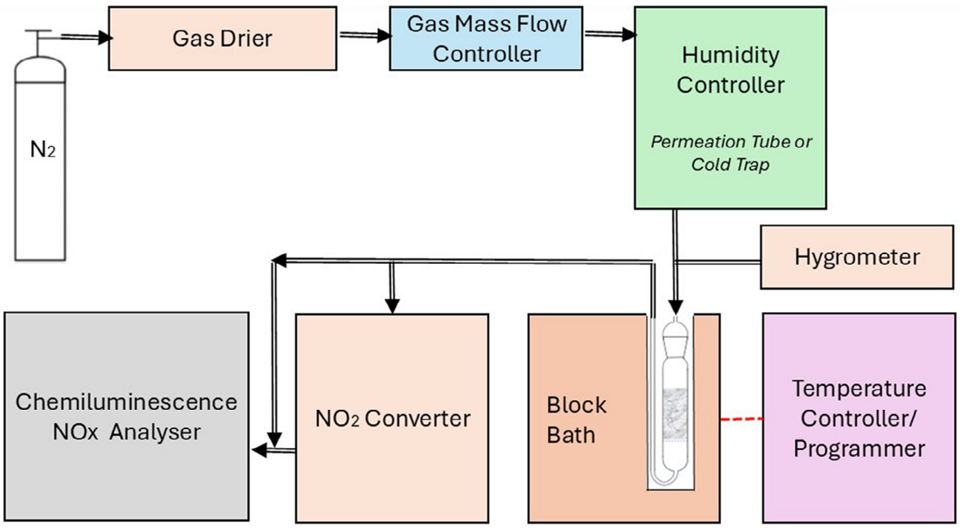

FIGURE 2 | Chemiluminescence flow experimental facility.

the temperature of which is controlled by a Eurotherm programmable temperature controller. The carrier gas BOC Zero Grade Nitrogen is passed through a Molecular Sieve 4A trap to remove moisture from the carrier gas. Flow control is achieved using an Omega FMA 2600A mass flow controller.

For experiments exploring the effect of moisture on decomposition rates, dry N_2 is passed through a permeation tube chamber, which can accommodate water permeation tubes that release water into the carrier gas stream at known rates. Fine-tuning of the rate of permeation is accomplished with a temperature-controlled tube oven. A Vaisala 152 dewpoint sensor measures the water content of the carrier gas flowing through the sample. The product gases from the decomposition are passed through an integral or external NO_2 converter to generate the NO detected by the NO_x analyser.

Two different NO_x analysers have been employed for these studies: (i) Seivers 280i NO analyser, which can detect less than one ppb NO and has a response speed of 200 ms. It operates at a low flow rate range (25–50 mL.min^{-1}), enabling all of the gas that passes through the sample to be passed into the analyser. The instrument does not have an integrated NO_2 converter and, hence, has been used to determine NO evolution rates only. (ii) Teledyne 200UP, with an integral NO_2 photolytic converter, can measure ppt levels of NO and NO_X and hence NO_2 by difference. The instrument inlet flow requires around 1000 mL.min^{-1} so two mass flow controllers are used to allow the sample gas stream of 40 mL.min^{-1} to combine with a diluent flow of pure N_2 before analysis.

3 | Results and Discussion

3.1 | NO_X Gases

There is wide agreement that the initial mode of decomposition of NC is through homolysis of the O—NO_2 bond to initially create gaseous NO_2. However, the dominant species observed by the chemiluminescence method is NO. This is consistent with the observations of others [10].

3.2 | Initial NO_X Evolution

Several authors have reported that on initial heating of NC, there is an initial high rate of evolution that eventually falls to a steady evolution rate. This was known by Will as Grenzzustand [16]. It is believed that this steady evolution rate is characteristic of the underlying stability of the material.

The initial high evolution rate was shown by Wallace [11] to depend on the history of the material prior to heating. Samples of NC were withdrawn from 25% water-wet storage in temperature-controlled magazines after intervals of 6, 26 and 58 months. After drying, the quantity of NO_X evolved from each sample was measured over a period of 40 min by chemiluminescence NO_x Analysis and it can be seen from Figure 3 to depend on the age of the material.

The quantity of NO_X evolved was also the determinant of the low observed heat test results. Whilst storage time had a significant impact on the Abel test, it had a minimal impact on the Bergman Junk results. This is consistent with Will's Grenzzustand hypothesis [13].

Table 3 shows the number of moles of NO_x evolved from each of the aged NC samples over the 40-min period when heated at 76.7°C. It includes the Bergman Junk test results, which were satisfactory, and the Abel heat test results, which failed for the samples stored for 26 and 58 months, respectively.

Volgelsanger [1] and Katoh [22] have made similar observations. They reported a correlation between low heat test results and a peak in the NO_x evolution rate when the sample was first heated. This has been attributed to NO_x being physically desorbed from the NC at the commencement of NO_X tests.

It has been thought that heating causes this desorption. However, in the chemiluminescence studies in our laboratory, the NO_x is displaced as soon as a carrier gas is passed through the NC at ambient (20°C) prior to heating the sample. Figure 4 shows the NO_x evolution from 5 g of NC (12.6%) when carrier gas is passed through the sample at an ambient temperature (~20°C).

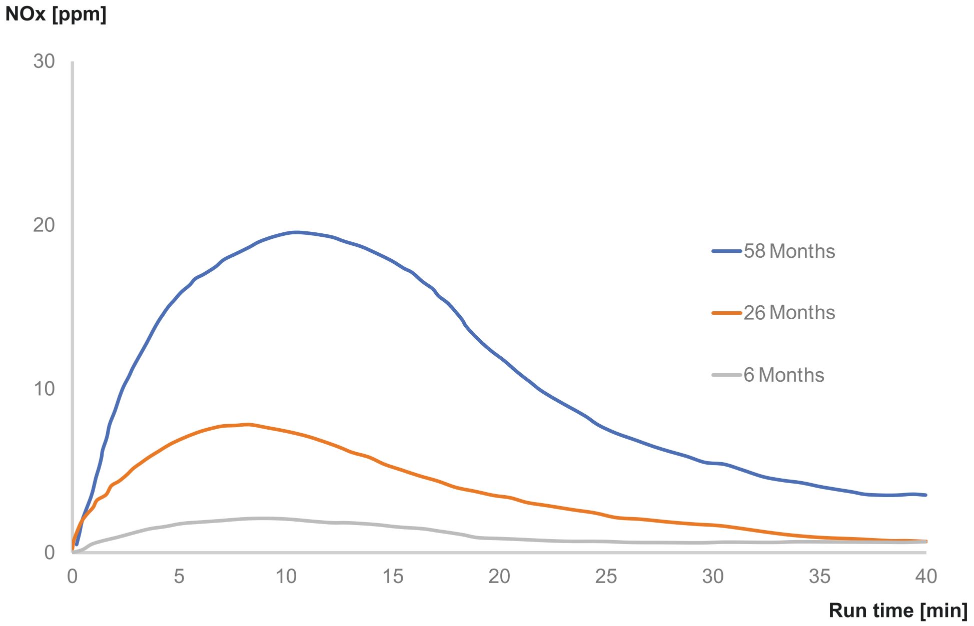

FIGURE 3 | Nitrogen oxides (NO_x) evolution at 76.7°C over a 40-min period from 1 g nitrocellulose (NC) (12.7%) samples stored wet at room temperature from 6 to 58 months.

TABLE 3 | Comparison of the nitrogen oxides (NO_x) evolved from nitrocellulose (NC) (12.7%) samples after wet storage for 6, 26 and 58 months with results from Bergman Junk and Abel tests.

Storage [month]	Moles NO_x [μmol]	Bergmann Junk [mL/g of NO]	Abel Heat Test [min]
6	0.0485	N/A	>30
26	0.165	0.90	6.7
58	0.478	0.97	4.5

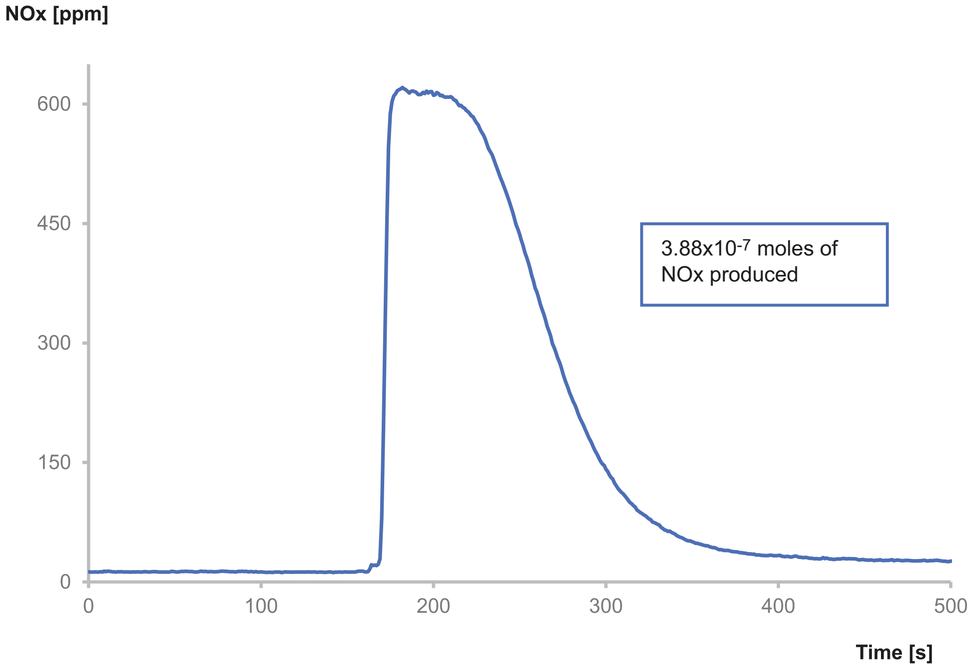

FIGURE 4 | Nitrogen oxides (NO_x) Evolved from 5 g nitrocellulose (NC) (12.6%) at the commencement of gas flow at ~20°C. The area under the curve was used to calculate the corresponding number of moles of NO_x generated.

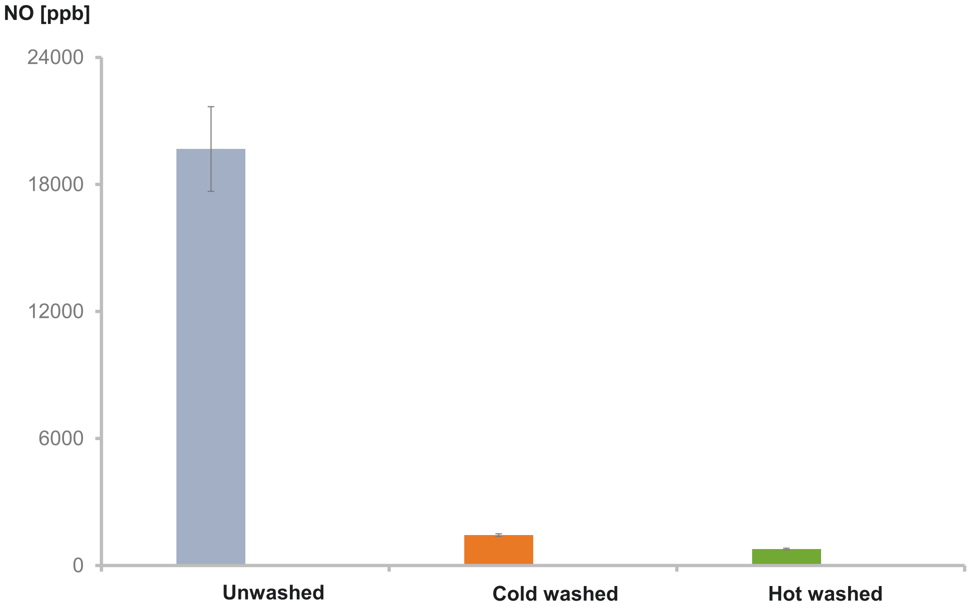

FIGURE 5 | Headspace injections from 5-year-old washed and unwashed nitrocellulose (NC) at ambient temperature.

A slightly different method of sampling was also used when the sample vessel was closed for a few minutes, allowing the gaseous products to accumulate in a low-volume reactor. Whilst the reactor is closed, the carrier gas is redirected into the analyser. After a few minutes, the reactor headspace is switched back into the sample flow of the chemiluminescence reactor, allowing the headspace to be analysed. In this method, a peak is observed with an area corresponding to the quantity of NO in the headspace of the reactor.

For these experiments, 20 mg dry samples of a 5-year-old NC (12.6%) that had been stored 25% water wetted at 5°C were inserted into the reactor at room temperature. This was closed for 15 min and then the headspace was injected into the chemiluminescence sample stream. Five samples were used. The peaks observed are from adsorbed NO_x that is being desorbed into the headspace of the reactor when the reactor is closed.

Further samples of the unwashed NC were then subjected, in one case, to washing with cold deionised water and in another, to boiling in deionised water for 3 min. Both samples were dried before being tested in the same way as the unwashed samples. Samples of 20 mg generated an almost undetectable level of NO, so the sample weights were adjusted to 60 mg for washed material and 80 mg for boiled material. The results, normalised for 100 mg, are shown in Figure 5.

Studies on adsorbed NO_x suggest that it can be readily released by heating the NC. Volltrauer et al. [10] suggested the activation energy for the desorption was around 58 $kJ.mol^{-1}$, while Wallace [11], Katoh et al. [22] and Vogelsanger [1] have all seen evidence of this desorption when heat is applied to the NC during the Abel heat test.

However, the current study suggests that the adsorbed material can be readily displaced by passing gas through the sample, by subjecting the sample to a vacuum or by washing the sample.

3.3 | Kinetic Studies

Having concluded that the early high evolution rates are due to the desorption of NO_x from the NC fibres, the main purpose of this work was to determine how temperature and moisture affect the decomposition over a range of temperatures from ambient to 135°C.

NC samples are prepared by drying the NC at 30°C in a vacuum oven for two days and subsequently keeping it in a desiccator for further use. This would have been effective in removing adsorbed material. The block oven was programmed to heat from ambient to a constant 30°C and held at that temperature for 2 h. At that point, the temperature was programmed to rise at a linear rate of $3°C.h^{-1}$ to 120°C and held at this temperature for a further 2 h. Samples (5 g of NC) were placed in the high-volume flow reactor. As the temperature was increased NO_x concentrations were measured for each second. The result for NC (12.6%) heated is shown in Figure 6.

As previously observed by Volltrauer et al. [10] and Wallace et al. [11], the Arrhenius plot is non-linear and can be resolved into two distinct lines with different gradients suggesting two different mechanisms with different activation energies. However, it is important to note that this result was obtained using a single carrier gas flow rate, a single mass of material and a single reaction vessel geometry.

The results were very reproducible, especially in the higher temperature regime (>70°C). At the lowest temperatures (<50°C), there was greater variability due to the very low concentrations of NO_x near the detection limits of the analyser and due to some variability in NO_x levels in the N_2 carrier gas. Understanding the factors that could affect the results such as sample mass, gas flow rate through the reactor and sample, and the compaction of the fibrous NC is crucial.

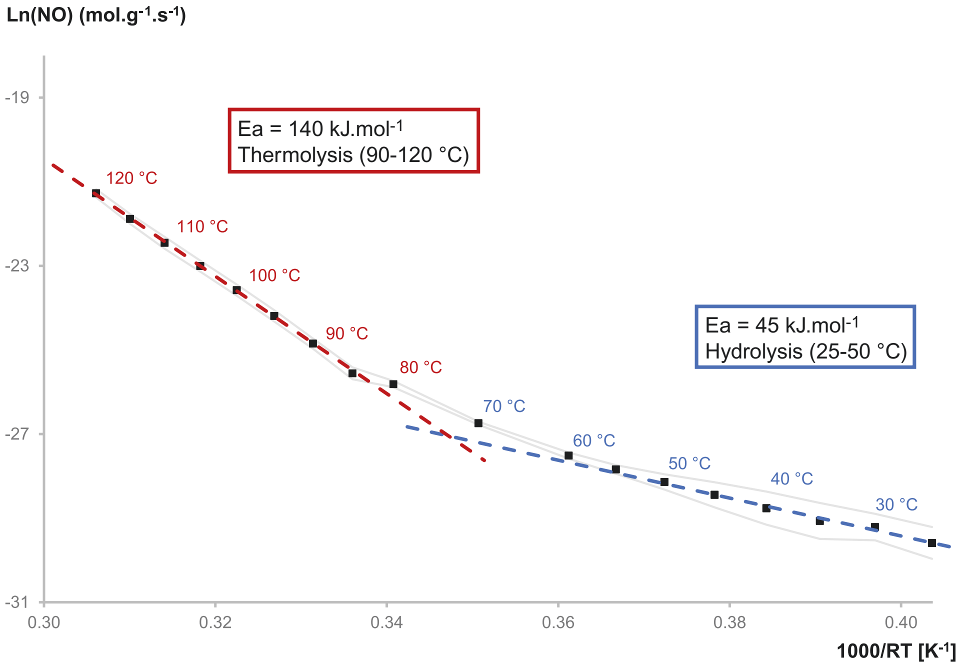

FIGURE 6 | Arrhenius plots for 5 g nitrocellulose (NC) (12.6%) at carrier gas flow rate of 30 mL/min. The red line represents the best fit for the data acquired from 90°C to 120°C, while the blue line represents the best fit for the data acquired from 25°C to 50°C. The two grey dotted lines indicate ± one standard deviation for the four replicates at each temperature.

3.4 | Arrhenius Plots–Effect of Sample Mass, Flow Rate and Sample Path Length

Arrhenius plots for the same NC samples were obtained where the mass of NC was reduced to 2.1 g, where the high and low-volume reactors were used and where the degree of compaction of the sample was varied. None of these significantly changed the values of activation energies and pre-exponential factors.

Experiments were also conducted to determine the effect of carrier gas flow rate. Will showed this to affect his results. At a flow rate that is too high, the gas stream can reduce the sample temperature, whilst, at a flow rate that is too low, the product gases can back-react with the NC. Through these experiments, an optimum flow rate of 40 ± 20 mL.min^{-1} was adopted for all subsequent experiments. This provided a consistent and reliable means of assessing the decomposition behaviour of NC.

3.5 | Arrhenius Plots–Effect of Moisture

Two mechanisms have been suggested to explain the two distinct slopes in the Arrhenius plots. The steeper slope has been attributed to the thermolysis mechanism, whilst the lower temperature slope has been attributed to the hydrolysis mechanism. A series of experiments were conducted to determine what effect changing the moisture content of the carrier gas has on the Arrhenius plots for 12.6% NC.

Several methods were used to control the moisture content of the N_2. In the first method, water permeation tubes with different permeabilities allowed moisture to be introduced into the gas stream. The humidity was fine-tuned by controlling the permeation tube's temperature. A baseline experiment was conducted at the lowest minimum achieved water concentration of 2 ppm. This was achieved by passing the carrier gas through a cold trap at −77°C. With this stream of dry $N_{2,}$ the NC temperature was ramped in 10°C increments from 30°C–100°C and the average NO concentration was determined. The Arrhenius plot in Figure 6 was constructed, showing the distinct slopes for the thermolysis and hydrolysis at 2 ppm water content.

Subsequent experiments were conducted where the humidity was held at a specific value whilst monitoring the NO_x evolution rate.

The results for 2 and 900 ppm water content show that in the higher thermolysis region, the increased humidity had little effect on the evolution rate of NO_x or on the Arrhenius parameters. At lower temperatures, moisture increases the rate of NO evolution but only has a small effect on the activation energy. At the NC temperature of ~60°C the NO evolution rate is 83% higher at 900 ppm H_2O than it was at 2 ppm.

In a second series of experiments, the humidity was controlled by passing the carrier gas through a glass bead-filled cold trap, which was kept in a freezer with a minimum temperature of −80°C. In this case, the NC was maintained at a constant temperature of 60°C. The freezer was allowed to warm naturally over a period of 10 h, allowing the moisture content to increase to a maximum of around 2600 ppm as measured with the in-line dew point sensor. The results for NC heated at 60°C are shown in Figure 8.

Again, there is a significant rise in the NO_x evolution rates. The rise in NO evolution rate is around 80% at 900 ppm water concentration. This is similar to that observed from the Arrhenius plot in Figure 7.

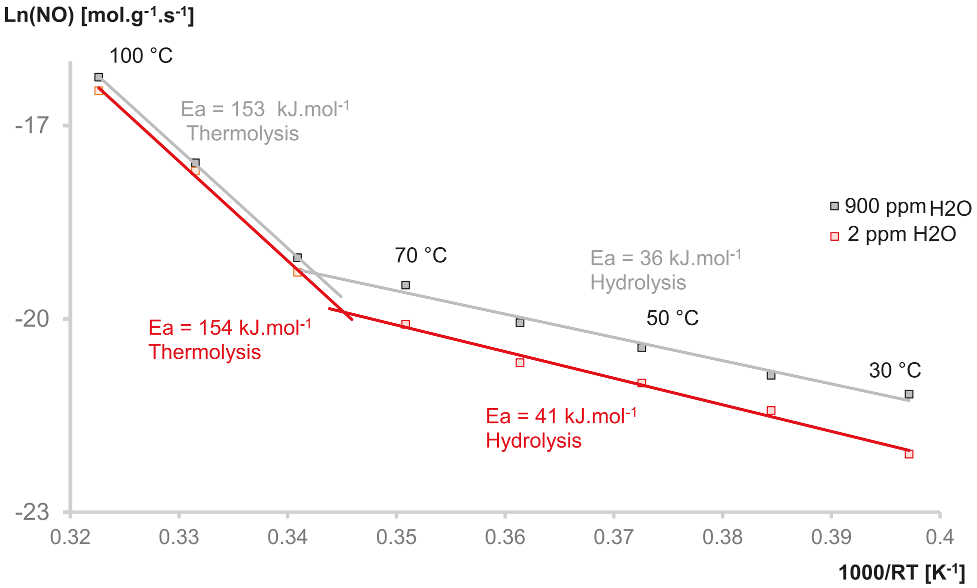

FIGURE 7 | Effect of moisture on 5 g nitrocellulose (NC) (12.6%) at carrier gas flow rate of 30 mL/min. The orange and grey solid lines represent the best fit for the data acquired from 30°C to 100°C for 2 and 900 ppm water (H_2O), respectively.

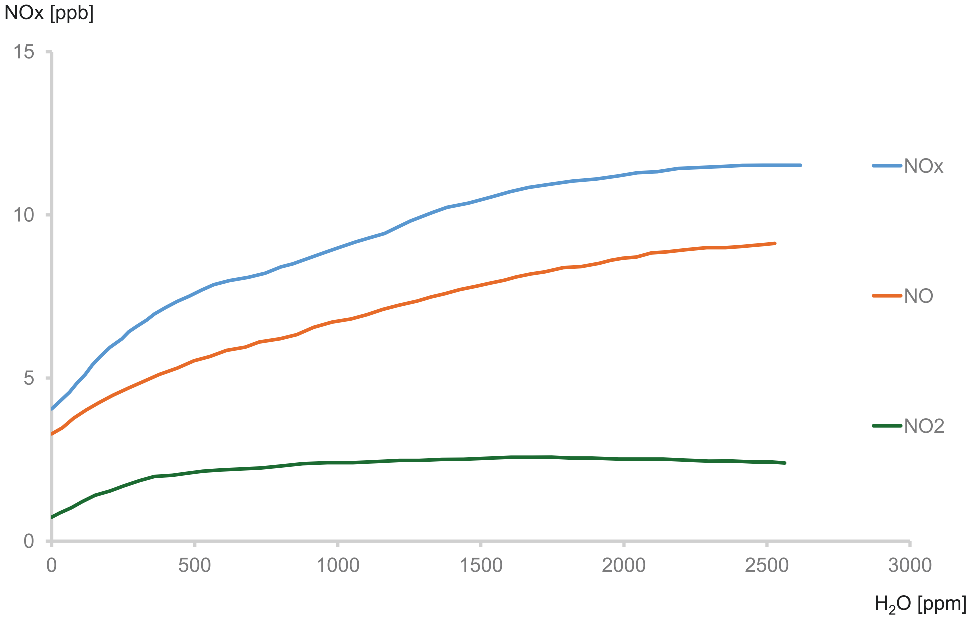

FIGURE 8 | Nitrogen oxides (NO_x) evolution from 5 g nitrocellulose (NC) sample(12.6%) heated at 60°C with a carrier gas flow rate of 40 mL/min.

4 | Conclusions

Chemiluminescence NO_x analysis has proven to be a powerful tool for exploring low-temperature decomposition behaviours of NC and formulations containing NC. By using an inert carrier gas (N_2) to sweep decomposition products into the analysers this method effectively can detect and measure NC degradation at temperatures at which NC and NC products are stored and used.

This work confirms that there are three major modes of NO_x evolution from NC, namely thermolysis, hydrolysis and desorption.

Thermolysis is the dominant mode of NO_x evolution at temperatures above 80°C and does not appear to be significantly influenced by the presence of moisture in the open flow situation that the current work has employed. In this higher temperature regime, hydrolysis continues to make a contribution to NO_X evolution, but this is masked by the very much greater contribution made by thermolysis. The activation energy for this mode of decomposition is 140 kJ.mol^{-1}. As the temperature reduces the hydrolysis mechanism plays an increasing role in the NO_x evolution rate and hence in the NC decomposition rate. At temperatures near or, a little above ambient, hydrolysis is the dominant mode of decomposition. Thermolysis continues to contribute to NO_x evolution rates, but this becomes negligible as temperatures decrease. The activation energy for this mode of decomposition is 46 kJ.mol^{-1}. These two different mechanisms, with their different activation energies, have an impact on life prediction and the concept of artificial ageing. If testing or gas analysis is carried out at elevated temperatures, then thermolysis plays a dominant role, so extrapolating to lower temperatures would underestimate the rate of decomposition of NC, which is being driven by hydrolysis. It is suggested that extrapolation to normal storage temperatures utilises the lower activation energy for temperatures below 60°C. Measuring stabiliser depletion is an indirect method of monitoring NC decomposition. Its use to predict ambient temperature decomposition rates needs to take into account the lower temperature kinetic behaviour and decmposition mechanism observed in this study.

The moisture content of the carrier gas significantly impacts NO_x evolution in the lower temperature domain. As the moisture content increases so too does the NO_x evolution rate. It is assumed that water in the gaseous phase equilibrates with water in the fibres of the NC. An increase in water concentration from 10 to 500 ppm caused a near doubling of the NO_x evolution rate from the NC. As the humidity level increases further to 2500 ppm the NO_2 rate evolution appears to level off whilst the NO evolution rate continues to increase although at a decreasing rate. The reason for the different behaviour is not yet understood.

Desorption or ‘prompt’ NO_x is a physical effect, releasing previously generated NO_x trapped within, or on the surface of NC. This source of NO_x is not directly influenced by the presence of moisture in the N_2 carrier gas.

With regards to stability testing, this work confirms that the Abel heat test is not a suitable test of the intrinsic stability of NC. Rather, it is a means by which the quantity of adsorbed NO_x can be assessed. This adsorbed material may be detrimental to the NC and formulations which use it and hence the Abel test and the chemiluminescence method have utility in revealing how much of this adsorbed material is present. Where the NC is to be incorporated into a formulation, it might be prudent to ensure that any adsorbed NO_x is removed prior to use since it might contribute to stabiliser depletion or other modes of degradation. This can be accomplished by washing, streaming gas through the material, or placing it under a vacuum.

This novel exploitation of the chemiluminescence technique has significant implications for the storage and handling of NC and formulations containing NC. Understanding the main decomposition mechanisms, at various temperatures, allows for more accurate life predictions and stability assessments and therefore improved safety protocols and storage guidelines.

Data Availability Statement

The data that support the findings of this study are available on request from the corresponding author. The data are not publicly available due to privacy or ethical restrictions.

References

1. J. Akhavan, *The Chemistry of Explosives* (London: The Royal Society of Chemistry, 2004).

2. T. Höfer, A. Rössler, and O. I. Strube, “Thermal Debonding on Demand for Wood Coatings via Nitrocellulose-based Primer,” *Progress in Organic Coatings* 188 (2024): 108215, https://doi.org/10.1016/j.porgcoat.2024.108215.

3. M. Lisiecki, T. G. A. Belé, S. Ügdüler, et al., “Mechanical Recycling of Printed Flexible Plastic Packaging: The Role of Binders and Pigments,” *Journal of Hazardous Materials* 472 (2024): 134375, https://doi.org/10.1016/j.jhazmat.2024.134375.

4. K. Haraguchi, S. Shimizu, and S. Tanaka, “Instant Strong Adhesive Behavior of Nanocomposite Gels Toward Hydrophilic Porous Materials,” *Langmuir* 34 (2018): 8480–8488, https://doi.org/10.1021/acs.langmuir.8b01448.

5. B. D. Grant, C. E. Anderson, J. R. Williford, et al., “SARS-CoV-2 Coronavirus Nucleocapsid Antigen-Detecting Half-Strip Lateral Flow Assay Toward the Development of Point of Care Tests Using Commercially Available Reagents,” *Analytical Chemistry* 92 (2020): 11305–11309, https://doi.org/10.1021/acs.analchem.0c01975.

6. E. A. Carter, B. Swarbrick, T. M. Harrison, and L. Ronai, “Rapid Identification of Cellulose Nitrate and Cellulose Acetate Film in Historic Photograph Collections,” *Heritage Science* 8 (2020): 51, https://doi.org/10.1186/s40494-020-00395-y.

7. J. Wang, G. Fu, and M. Yan, “Comparative Analysis of Two Catastrophic Hazardous Chemical Accidents in China,” *Process Safety Progress* 39 (2020): e12137, https://doi.org/10.1002/prs.12137.

8. Q. Chen, M. Wood, and J. Zhao, “Case Study of the Tianjin Accident: Application of Barrier and Systems Analysis to Understand Challenges to Industry Loss Prevention in Emerging Economies,” *Process Safety and Environmental Protection* 131 (2019): 178–188, https://doi.org/10.1016/j.psep.2019.08.028.

9. B. Vogelsanger, “Chemical Stability, Compatibility and Shelf Life of Explosives,” *Chimia* 58 (2004): 401–408, https://doi.org/10.2533/000942904777677740.

10. H. N. Volltrauer and A. Fontijn, “Low-temperature Pyrolysis Studies by Chemiluminescence Techniques Real-time Nitrocellulose and PBX 9404 Decomposition,” *Combustion and Flame* 41 (1981): 313–324, https://doi.org/10.1016/0010-2180(81)90065-1.

11. I. G. Wallace and R. G. Powell, “The Application of a Chemiluminescence NOx Analyser to Stability Testing,” Paper Presented at *Proceedings of the International Annual Conference on Information and Communication Technology*, (Karsruhe, 1980): 195–217.

12. R. W. Phillips, C. A. Orlick, and R. Steinberger, “The Kinetics of the Thermal Decomposition of Nitrocellulose,” *Journal of Physical Chemistry* 59 (1955): 1034–1039, https://doi.org/10.1021/J150532A011.

13. W. Will, *Jaresbericht Der Zentralstelle Fur wissenschaflich-Technische Untersuchungen* (1900).

14. G. M. Khrapkovskii, T. F. Shamsutdinov, D. V Chachkov, and A. G. Shamov, “Energy of the O–NO_2 Bond Dissociation and the Mechanism of the Gas-Phase Monomolecular Decomposition of Aliphatic Alcohol Nitroesters,” *Journal of Molecular Structure: THEOCHEM* 686 (2004): 185–192, https://doi.org/10.1016/j.theochem.2004.09.001.

15. T. B. Brill and P. E. Gongwer, “Thermal Decomposition of Energetic Materials 69. Analysis of the Kinetics of Nitrocellulose at 50°C–500°C,” *Propellants, Explosives, Pyrotechnics* 22 (1997): 38–44, https://doi.org/10.1002/prep.19970220109.

16. J. Kimura, “Chemiluminescence Study on Thermal Decomposition of Nitrate Esters (PETN and NC),” *Propellants, Explosives, Pyrotechnics* 14 (1989): 89–92, https://doi.org/10.1002/prep.19890140302.

17. A. R. Jabalquinto, N. Mai, S. Belghiche, and P. P. Gill, “Modified Arrhenius Kinetics for Double Base Propellant Decomposition: Effect of

Water,” *Polymer Degradation and Stability* 227 (2024): 110846, https://doi.org/10.1016/j.polymdegradstab.2024.110846.

18. H. N. Volltrauer, “Real Time Low Temperature Decomposition of Explosives—PETN,” *Journal of Hazardous Materials* 5 (1982): 353–357, https://doi.org/10.1016/0304-3894(82)85023-1.

19. R. Tunnell, R. Dale, I. King, and D. Tod, “Using Thermal Methods to Understand the Interactions Between a Rocket Propellant and Igniter Material,” *Journal of Thermal Analysis and Calorimetry* 131 (2018): 379–395, https://doi.org/10.1007/s10973-017-6830-2.

20. B. A. McDonald, “Study of the Effects of Aging Under Humidity Control on the Thermal Decomposition of NC/NG/BTTN/RDX Propellants,” *Propellants, Explosives, Pyrotechnics* 36 (2011): 576–583, https://doi.org/10.1002/prep.200900094.

21. F. P. Teixeira, A. C. Anastacio, L. G. de Mendonça-Filho, and J. Nichele, “Effect of Relative Humidity and Absorbed Water on the Ethyl Centralite Consumption in Nitrocellulose-based Propellants,” *Cellulose* 30 (2023): 1411–1420, https://doi.org/10.1007/s10570-022-04999-4.

22. K. Katoh, S. Fukui, A. Haba, E. Higashi, T. Saburi, and K. Okada, “Comparison Between Abel Test Stability and Thermal Decomposition Behavior of Nitrocellulose,” *Journal of Thermal Analysis and Calorimetry* 147 (2022): 7563–7571, https://doi.org/10.1007/s10973-021-11043-3.

The use of chemiluminescence nitrogen oxides analysis for the study of the decomposition of nitrocellulose

Wallace, Ian G.

2025-05

Wallace I, Mai N, Gill P, et al., (2025) The use of chemiluminescence nitrogen oxides analysis for the study of the decomposition of nitrocellulose. Propellants, Explosives, Pyrotechnics, Volume 50, Issue 5, May 2025, Article number e12040

https://doi.org/10.1002/prep.12040